Nigerian Research Journal of Engineering and Environmental Sciences 7(1) 2022 pp. 319-329
p ISSN: 2635-3342; e ISSN: 2635-3350

Nigerian Research Journal of Engineering and Environmental Sciences
Journal homepage: www.rjees.com

Original Research Article

Speed Control of Direct Current Motors

***Onah, A.J., Awah, C.C. and Diyoke, G.C.**

Department of Electrical/Electronic Engineering, College of Engineering and Engineering Technology, Michael Okpara University of Agriculture, Umudike, Abia State, Nigeria.
*aniagbosoonah@yahoo.com

http://doi.org/10.5281/zenodo.6786613

ARTICLE INFORMATION

Article history:
Received 13 Mar, 2022
Revised 23 Apr, 2022
Accepted 23 Apr, 2022
Available online 30 Jun, 2022

Keywords:
DC motors
Variable-speed drives
Fully-controlled rectifier
Delay-angle
Torque
Armature-voltage control
Field control

ABSTRACT

Direct current (DC) motors are used in variable-speed drives to produce a high starting torque, and provide speed control over a wide range of speed. Controlled rectifiers are popularly employed in the speed control of DC motors. In this paper, the speed control of separately excited dc motor, using single-phase, full-wave, fully-controlled rectifier was investigated. Controlled rectifiers were used to produce variable DC output voltages from a fixed alternating current (AC) voltage. Since the armature voltage (V_a) of a DC motor is the output of a single-phase controlled rectifier, it was varied by varying the delay or firing angle (α_a) of the rectifier. The field circuit also requires a rectifier to control the field current (I_f) or flux by varying the firing angle (α_f). In this paper, the motor speed equations were derived. The output equations of the rectifiers were also derived and incorporated into the motor speed equations. The graphs generated from these equations show clearly how the speed of the DC motor varies with the output voltage or current of the controlled rectifiers. Thus, motor speed, being a function of the armature voltage (V_a), or the field current (I_f) was controlled. This paper demonstrates the control strategies of a separately excited dc motor, using single-phase controlled rectifiers.

1. INTRODUCTION

A direct current (DC) motor is a machine that converts DC electrical energy into rotating mechanical energy. They are rated in horsepower. They find wide applications in dc drive systems for paper production, photographic film manufacturing, machine tools, traction, crude oil pipelines, variable-speed drives for woodworking machines, adjustable-speed drive systems for textiles (Traister, 1992; Sen, 1995). Like other electrical apparatus, DC motors depend on the principles of magnetism for their operation. If current is

passed through a conductor or wire situated in a magnetic field, a force is exerted on the conductor, moving it through the magnetic field. If the conductor is moved in such a way that the conductor cuts across the lines of flux, an electromotive force (EMF) is induced in that conductor. If the conductor remains stationary while the magnetic field moves so that its lines cut across the conductor, an EMF will be induced in the conductor.

DC motors are widely employed where speed variation, good speed regulation, frequent starting, braking, and reversing are required. To achieve these goals, the motor speed is usually controlled. Before the advent of power electronic converters, electric motor drives were implemented with electromechanical devices such as contactors, push buttons, solenoids, motor starters, electromechanical relays, resistors, coils, pneumatic timing devices e. t. c. Here resistance control is usually the method of speed control implemented - a variable resistor is placed in series with the armature or field circuit to vary the current, and control the speed of the motor. The resistance control method has poor efficiency and is no longer popular. In modern motor drive speed control, power electronics converters are generally applied (Chang et al., 2016). In DC motor speed control, these converters are used to control the armature voltage or the field current. Hence the methods of speed control known as armature voltage control and field flux control are applied. Armature voltage control is adopted when the motor runs at speed less than the rated motor speed. In this case the armature current and field current are held constant, while the armature voltage is varied to control the motor speed. For speeds higher than the rated speed, the armature voltage is maintained constant at rated value and the field current is varied to control the speed. Therefore, this paper focuses on the application of the armature voltage control and the field current control methods. In this paper, the power electronic converter employed is a rectifier. Thus, the paper shows how the speed of rotation of the dc motor is controlled, using single-phase, full-wave and fully-controlled rectifiers.

2. METHODOLOGY

2.1. The Operation of the DC Motor

Figure 1 is the steady-state equivalent circuit of the separately excited DC motor. The field and armature voltages were controlled independent of each other. Thus, when electric current (I_f) flows in the field winding, the magnetic field created exerts a force on the rotor or armature coils carrying the current (I_a), causing it to rotate. A voltage, E known as back EMF is induced in the armature winding as it rotates. V_a and R_a are the terminal voltage and the resistance respectively of the armature circuit.

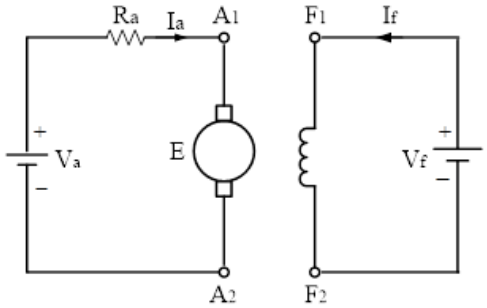

Figure 1: Separately excited DC motor

From Figure 1, the basic equations of the DC motor for steady-state operation were derived as follows:

$$V_a = R_a I_a + E \tag{1}$$

It can be shown that the relationship between the generated EMF, speed, flux, and the number of conductors in the armature is:

$$E = \frac{pZ}{c}\frac{2\pi N}{60}\phi = k\phi\omega_m = K\omega_m \quad (2)$$

The flux (ϕ) is proportional to the field current (I_f), therefore:

$$E = kI_f\,\omega_m = K\omega_m \quad (3)$$

$$\omega_m = \frac{2\pi N}{60} \quad (4)$$

Where p = number of poles, N = speed in rpm, ϕ = useful flux per pole entering or leaving the armature in Wb, Z = total number of armature conductors, c = number of parallel paths through winding between positive and negative brushes, Z/c=Number of conductors in series in each path and $k=Pz/c$ (constant of every machine).
From Equation (1), the total electrical power supplied to the armature is given by:

$$V_a I_a = R_a I_a^2 + EI_a \quad (5)$$

$R_a I_a^2$ = Loss due to resistance of armature circuit and EI_a= mechanical power developed by the armature.
From Equation (2):

$$EI_a = k\phi\omega_m I_a = T_a\omega_m \quad (6)$$

T_a = torque developed by the armature

From Equations (3) and (6):

$$T_a = KI_a \quad (7)$$

Equation (1) can be written as:

$$V_a = R_a I_a + K\omega_m \quad (8)$$

Thus:

$$\omega_m = \frac{V_a - R_a I_a}{K} \quad (9)$$

From Equations (7) and (9), the relationship between the motor speed and torque can be written as:

$$\omega_m = \frac{V_a}{K} - \frac{R_a}{K^2}T_a \quad (10)$$

2.2. Single-phase Fully-Controlled Rectifier

Figure 2 shows the circuit of a single-phase full converter and Figure 3 is the armature circuit (Kazuaki and Hirotaka, 2014; Mohammad et al, 2016; Agu, 2019). The load (motor) consists of a series resistance (*R)*, reactance (*L)*, and back EMF (*E)*. Figure 4 shows the supply voltage and the gate pulses applied to the switches. From Figure 4, switches S_1 and S_2 are forward biased during the positive half-cycle of the source

voltage (v_s) and when they are fired at $\omega t = \alpha$ (α is the delay angle of the rectifier), the load is connected to v_s and load current (i_a) flows until $\omega t = \pi + \alpha$ when the switches S_3 and S_4 are fired during the negative half-cycle of the source voltage (v_s). Because of the high inductive load, S_1 and S_2 continue to conduct beyond π though v_s has gone negative. As S_3 and S_4 are fired, S_1 and S_2 are forced to go off as a result of line or natural commutation. Trigger signal is $(\pi - \alpha)$ radians long all the time. A passive LC filter can be installed on the DC side to reduce voltage ripples, but due to its low resonance frequency, it increases the overall size, weight, and cost (Ismail, 2009; Maheshwari et al., 2013; Kazuaki and Hirotaka, 2014).

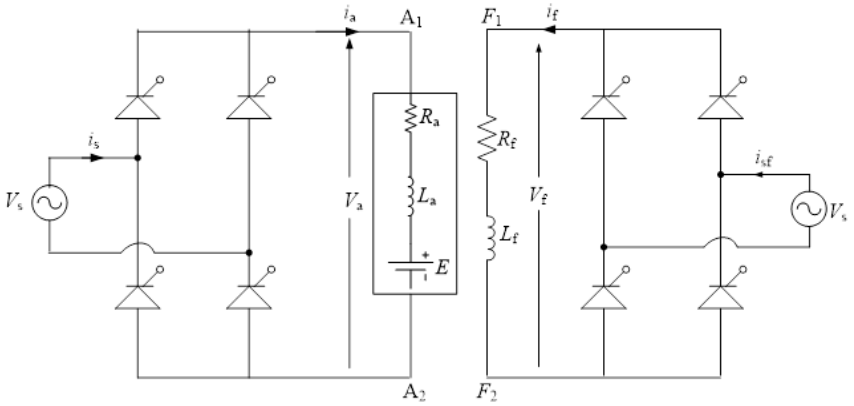

Figure 2: Single-phase full-converter drive

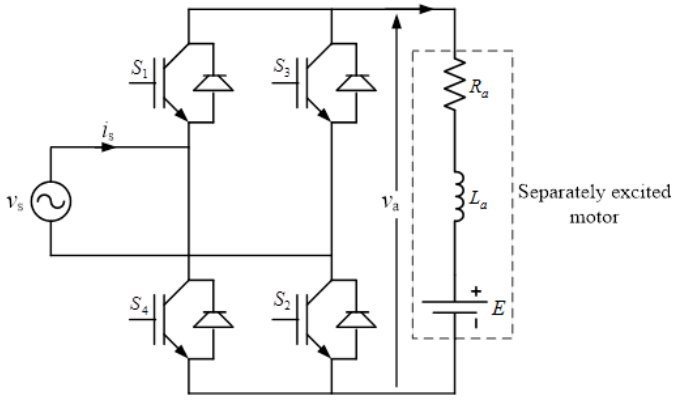

Figure 3: Single-phase full-bridge converter

In Figure 3, the supply voltage is v_s. With the switches on, v_a is the voltage drop across the series combination of *R*, *L* and *E*. The source voltage v_s is given by:

$$v_s = V_m \sin \omega t \tag{11}$$

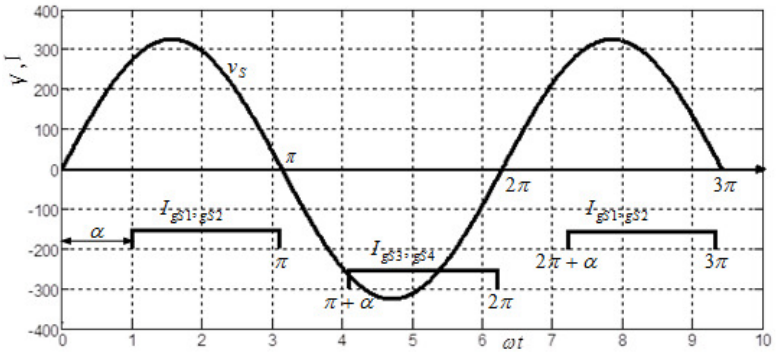

Figure 4: Supply voltage and switch gate pulses

In Fourier series, the output voltage, v_a for continuous current operation is expressed as:

$$v_a = \frac{a_o}{2} + \sum_{n=1}^{\infty} \left(a_n \cos n\omega t + b_n \sin n\omega t\right) \tag{12}$$

The Fourier coefficients (a_o, a_n and b_n) are derived as:

$$a_o = \frac{2}{\pi}\int_{\alpha}^{\pi+\alpha} V_m \sin \omega t \, d(\omega t) = \frac{4V_m}{\pi}\cos\alpha \tag{13}$$

$$a_n = \frac{1}{\pi}\left\{\int_{\alpha}^{\pi+\alpha} V_m \sin \omega t \, \cos n\omega t \, d(\omega t) - \int_{\pi+\alpha}^{2\pi+\alpha} V_m \sin \omega t \, \cos n\omega t \, d(\omega t)\right\} \tag{14}$$

$$a_n = \frac{2V_m}{\pi}\left[\frac{\cos(n+1)\alpha}{n+1} - \frac{\cos(n-1)\alpha}{n-1}\right] \qquad \text{n=2,4,6,…} \tag{15}$$

$$b_n = \frac{1}{\pi}\left\{\int_{\alpha}^{\pi+\alpha} V_m \sin \omega t \, \sin n\omega t \, d(\omega t) - \int_{\pi+\alpha}^{2\pi+\alpha} V_m \sin \omega t \, \sin n\omega t \, d(\omega t)\right\} \tag{16}$$

$$b_n = \frac{2V_m}{\pi}\left[\frac{\sin(n+1)\alpha}{n+1} - \frac{\sin(n-1)\alpha}{n-1}\right] \qquad \text{n=2,4,6,…} \tag{17}$$

Equations (13), (15) and (17) are combined to obtain the expression for v_a as:

Thus:

$$v_a = \frac{2V_m}{\pi}\cos\alpha + \sum_{2,4,6}^{\infty} \left(a_n \cos n\omega t + b_n \sin n\omega t\right) \tag{18}$$

$$i_a = I_a + \sum_{n=2,4,6,\ldots}^{\infty} \left(\frac{a_n}{Z_n}\cos(n\omega t - \theta_n) + \frac{b_n}{Z_n}\sin(n\omega t - \theta_n)\right) \tag{19}$$

$$I_a = \frac{V_a - E}{R} \tag{20}$$

$$Z_n = \sqrt{R_a^2 + (n\omega L_a)^2}\,; \quad \theta_n = \tan^{-1}\left(\frac{n\omega L_a}{R_a}\right)$$

2.3. Armature Voltage Control

Under steady-state conditions, the armature voltage is obtained from Equation (18) as:

$$V_a = \frac{2V_m}{\pi}\cos\alpha \tag{21}$$

This is the voltage applied across the motor armature terminals when the gate signal is applied to the rectifier switches, while being forward biased.
From Equations (9) and (21), the motor speed becomes:

$$\omega_m = \frac{1}{K}\left(\frac{2V_m}{\pi}\cos\alpha - R_a I_a\right) \tag{22}$$

With respect to the developed motor torque (T_a), the motor speed from Equation (10) becomes:

$$\omega_m = \frac{2V_m}{\pi K}\cos\alpha - \frac{R_a}{K^2}T_a \tag{23}$$

From Equation (23), the developed torque (T_a) is:

$$T_a = \frac{K^2}{R_a}\left(\frac{2V_m}{\pi K}\cos\alpha - \omega_m\right) \tag{24}$$

The usefulness of the motor lies in the value of the torque it can develop since it is the torque that drives the load. The torque developed by the motor consists of the average motor torque (T_a) produced by the DC component (average value) of the current (I_a) and the pulsating torque (T_n) produced by the AC current components (Allmeling, 2004).

$$T = T_a + T_n = KI_a + K\sqrt{\sum_{n=2}^{\infty} i_n^2} \tag{25}$$

2.4. Field Control

This control method is applied when the motor speed is to be increased beyond the base or rated value. Since the armature voltage cannot be increased above the rated value, it is maintained at the rated value, and the field current (I_f) is therefore increased by adjusting the delay angle (α_f) to control the speed. The following equations were derived from Figure 2: The field circuit voltage, V_f was obtained as:

$$V_f = \frac{2V_m}{\pi}\cos\alpha_f \tag{26}$$

The field current, I_f is:

$$I_f = \frac{V_f}{R_f} = \frac{2V_m}{\pi R_f}\cos\alpha_f \tag{27}$$

The back EMF (E) from Equation (3) is:

$$E = kI_f\,\omega_m \tag{28}$$

From Equation (28), the speed, ω_m of the motor is:

$$\omega_m = \frac{E}{kI_f} \tag{29}$$

The relationship between the armature current and the field current is given as:

$$I_a = \frac{V_a - kI_f\omega_m}{R_a} \tag{30}$$

Equation (7) becomes:

$$T_a = kI_f I_a \tag{31}$$

3. RESULTS AND DISCUSSION

The output voltage Equation (18) and the current Equation (19) were plotted in Figure 5. The rated values of the motor parameters are: $V_a = 200\,\text{V}$, $I_a = 20\,\text{A}$, $N_m = 1500\,\text{rpm}$, $R_a = 5\Omega$, $R_f = 120\Omega$, $L_a = 30\,\text{mH}$, Source voltage, $V_s = 230\,\text{V}$, $f = 50\,\text{Hz}$. It can be noticed in Figure 5 that the steady-state voltage across the motor armature is V_a and the average armature current is I_a.

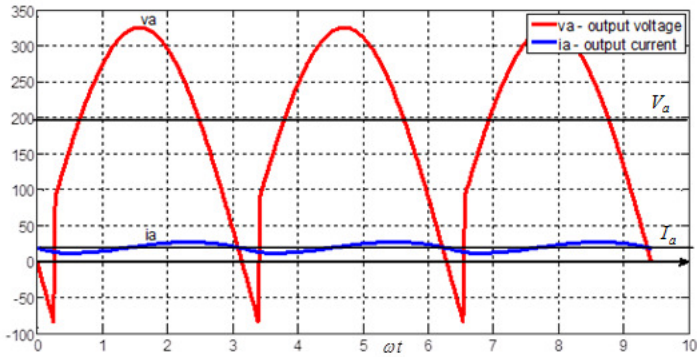

Figure 5: Output voltage and current waveforms of the rectifier in Figure 3

Equation (21) was plotted as shown in Figure 6. It shows how the output voltage (V_a) of the rectifier varies with the firing angle (α). The voltage is adjusted by decreasing or increasing the firing angle.

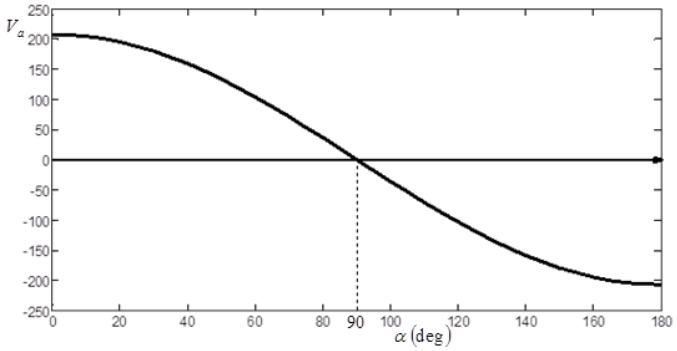

Figure 6: Output voltage (V_a) versus the firing angle (α)

The torque (T_a) developed by the motor, is shown in Figure 7. The average torque (T_a) is shown in the figure to be 12.73 N.m. The average value of T_n is zero.

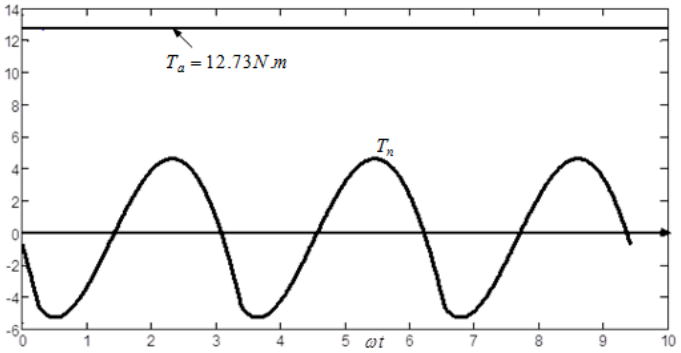

Figure 7: Torque developed by the motor

The armature voltage control equations derived in this paper were plotted as shown in Figures 8 to 10. The speed of the motor (ω_m) as a function of armature current (I_a) and voltage (V_a) is shown in Figure 8. As stated earlier, the speed of the motor can be controlled by varying the armature voltage (V_a). If the speed of the motor drops below rated value, the back EMF will also decrease, leading to the rise in armature current. So the value of the armature voltage, (V_a) must be reduced in order to prevent the current (I_a) from rising above rated value. Hence V_a is normally varied by varying the delay angle (α) of the rectifier. The speed of the DC motor varies directly with the armature voltage. It can be noted in Figure 8 that the motor attains its rated speed of 157 rad/s or 1500 rpm when the armature voltage (V_a) and current (I_a) reach rated values of 200 Vand 20 A respectively.

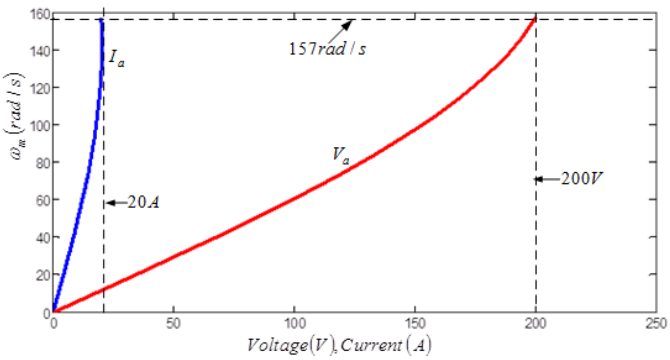

Figure 8: Speed of the motor (ω_m) versus I_a and V_a

Figure 9 is the plot of torque (T_a) versus current (I_a), and voltage (V_a). It shows that torque is directly proportional to current and voltage. It can be observed in Figure 9 that the load connected to the motor should not exceed 12.73 N.m because this is the maximum torque that can be developed by the motor at the rated armature voltage (V_a) and current (I_a) of 200 V and 20 A respectively.

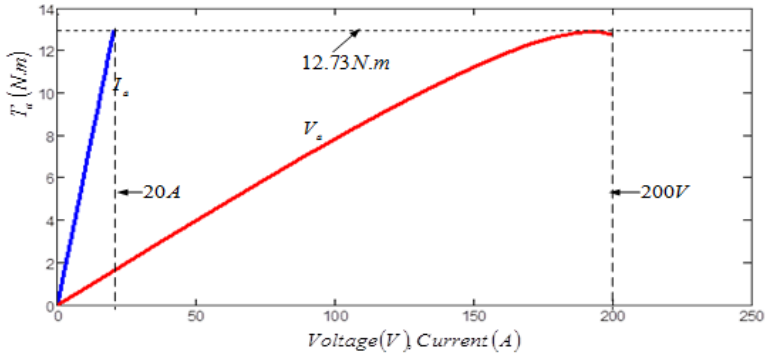

Figure 9: Torque versus current and voltage

Figure 10 is the plot of speed versus torque. When the armature voltage is increased, the armature current increases, leading to the increase in torque, and consequently, rise in speed. Figure 10 shows that the maximum torque obtainable from the motor is 12.73 N.m. at the rated speed of 157 rad/s.

The field control equations derived in the preceding section were plotted as shown in Figures 11 to 13. Figure 11 is the plot of speed versus field current. If the field voltage is increased by adjusting the delay angle, field current increases, leading to increase in the back EMF, and consequently speed rises. This can be observed in Figure 11. As stated previously, motor speeds higher than the rated value can be achieved with field control, for example, a speed of 200 rad/s is obtained with field current of 2.76 A as shown in Figure 11. The rated speed (157 rad/s) was obtained with field current of 2.07 A. Figure 12 is the plot of torque versus field current. If the field current is increased by increasing the voltage through the adjustment of the delay angle, the back EMF increases, leading to decrease in armature current, and consequently torque decreases. The developed torque was 12.73 N.m as shown in the figure. Maximum torque was attained at field current of 2.07 A. Figure 13 is the plot of speed versus torque. As the speed of the motor increases the torque developed decreases proportionately (Traister, 1992). Motor speed increased by increasing the field current (I_f). The torque developed by the motor was 12.73 N.m. at the rated speed.

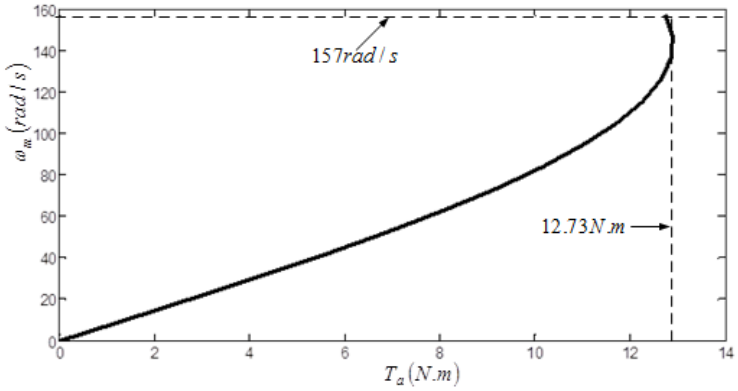

Figure 10 Plot of speed versus torque

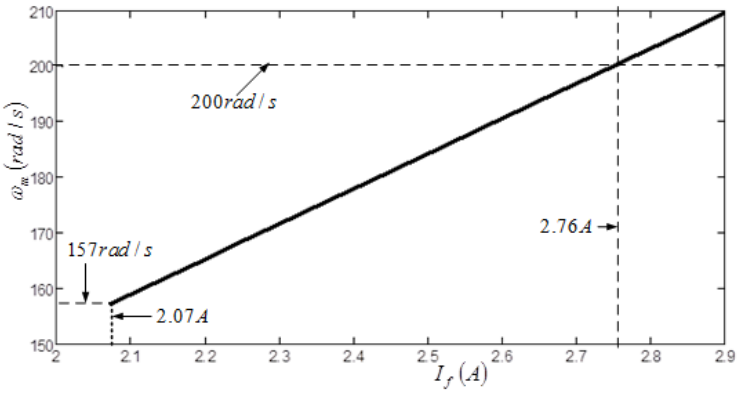

Figure 11: Plot of speed versus field current

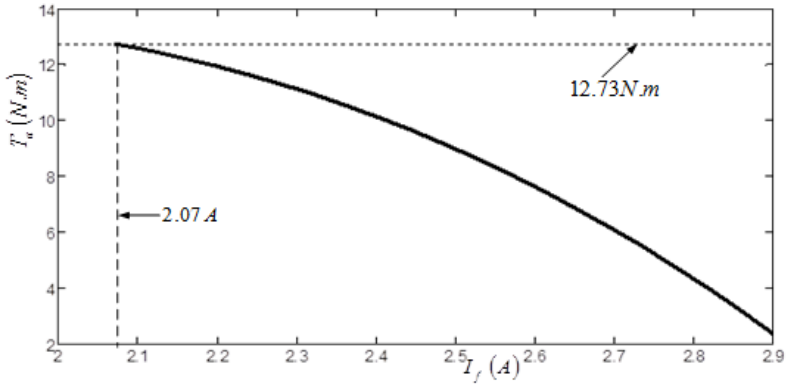

Figure 12: Plot of torque versus field current

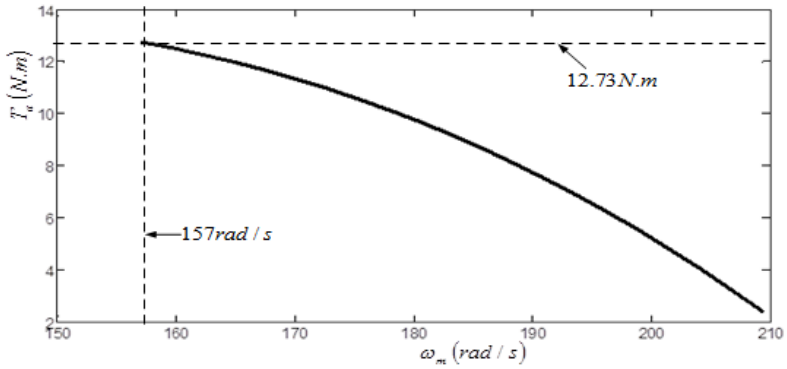

Figure 13 Plot of speed versus of torque

4. CONCLUSION

Speed control of separately excited DC motor has been investigated in this paper. Two methods of control – armature voltage control and field control are the most popular. The paper shows how DC voltage can be produced from an AC source, using single-phase, full-wave, fully-controlled rectifier. For armature voltage control, it can be noted that speed is directly proportional to voltage, current and torque. Torque is also directly proportional to voltage and current. The motor attains its rated speed of 157 rad/s when the rectifier

output voltage equals the motor rated voltage of 200 V and the rated current of 20 A flows. At these values of the motor variables, the motor develops a maximum torque of 12.73 Nm. By virtue of the armature voltage control, these values of speed and torque attained by the motor cannot be exceeded since the motor rated voltage of 200 V must not be exceeded. However, when speed is to be increased above rated speed, field control comes into play. As for the field control, speed is directly proportional to field current, torque is inversely proportional to field current, and speed is inversely proportional to torque. During field control, the motor rated speed of 157 rad/s and maximum developed torque of 12.73 Nm were achieved with field current of 2.07 A. Motor speed increases with increase in field current, while developed torque decreases with increase in field current. This is because the armature current which determines the torque decreases with increase in field current.

5. CONFLICT OF INTEREST

There is no conflict of interest associated with this work.

REFERENCES

Agu, M. U. (2019). *Principles of Power Electronic Circuits*, University of Nigeria Press, Enugu, pp. 237-253.

Allmeling, J. (2004). A control Structure for Fast Harmonics Compensation in Active Filters. *IEEE Transactions on Power Electronics,* 19(8), pp. 508-514.

Chang, Y.C., Chen, C. H., Zhu, Z. C. and Huang, Y. W. (2016). Speed Control of the Surface-Mounted Permanent-Magnet Synchronous Motor Based on Takagi-Sugeno Fuzzy Models. *IEEE Transactions on Power Electronics*, 31(9), pp. 6504-6510.

Hart, D. W. (1997). *Introduction to Power Electronics*. Prentice Hall Inc., pp. 125-132.

Ismail, F. C. (2009). Bridgeless Sepic Rectifier with Unity Power Factor and Reduced Conduction Losses. *IEEE Transactions on Industrial Electronics*, 56(4), pp. 1147-1157.

Kazuaki F. and Hirotaka K. (2014). Analysis of Half-Wave Class DE Low dv/dt Rectifier at Any Duty Ratio, *IEEE Transactions on Power Electronics*, 29(1), pp. 3657-3668.

Maheshwari, R., Munk-Nielsen, S. and Lu, K. (2013). An active damping technique for small DC-link capacitor based drive system*, IEEE Transactions on Industry Information*, 9(2), pp. 848-858.

Mohammad P., Ahmad A. A., Adib A. and Mohammad E. J. (2016). A Straightforward Procedure to Select Passive Elements in Single-phase Pulse-width Modulation Rectifiers with Developed Resonant Current Controller, *Electric Power Components and Systems*, 44(4), pp. 379-389.

Rashid, M. H. (1993). *Power Electronics: Circuits, Devices, and Applications*. Prentice Hall Inc., pp. 493-513.

Sen, P. C. (1995). Electric Motor Drives and Control: past, present and future. *IEEE Transactions on Industrial Electronics*, 37(6), pp. 562-575

Traister J.E. (1992). *Handbook of Electric Motors: Use and Repair*, 2nd Edition, The Fairmont Press Inc., pp. 1-8.